Applied Mathematical Modelling 34 (2010) 3659–3673

Contents lists available at ScienceDirect

Applied Mathematical Modelling

journal homepage: www.elsevier.com/locate/apm

Levy-type solution for buckling analysis of thick functionally graded rectangular plates based on the higher-order shear deformation plate theory

M. Bodaghi, A.R. Saidi *

Department of Mechanical Engineering, Shahid Bahonar University of Kerman, Kerman, Iran

ARTICLE INFO

Article history:
Received 23 November 2009
Received in revised form 10 March 2010
Accepted 15 March 2010
Available online 17 March 2010

Keywords:
Buckling analysis
Functionally graded
Thick rectangular plate
Higher-order shear deformation theory
Levy solution

ABSTRACT

In this article, an analytical approach for buckling analysis of thick functionally graded rectangular plates is presented. The equilibrium and stability equations are derived according to the higher-order shear deformation plate theory. Introducing an analytical method, the coupled governing stability equations of functionally graded plate are converted into two uncoupled partial differential equations in terms of transverse displacement and a new function, called boundary layer function. Using Levy-type solution these equations are solved for the functionally graded rectangular plate with two opposite edges simply supported under different types of loading conditions. The excellent accuracy of the present analytical solution is confirmed by making some comparisons of the present results with those available in the literature. Furthermore, the effects of power of functionally graded material, plate thickness, aspect ratio, loading types and boundary conditions on the critical buckling load of the functionally graded rectangular plate are studied and discussed in details. The critical buckling loads of thick functionally graded rectangular plates with various boundary conditions are reported for the first time and can be used as benchmark.

1. Introduction

In order to static and dynamic analysis of plate structures, a number of plate theories are available based on considering the transverse shear deformation of plate. The classical plate theory (CPT) in which the transverse shear deformation effects are neglected and the normal to the mid-plane remains straight and normal to the middle surface during the deformation. As a result, the classical plate theory usually underestimates deflection and overestimates the natural frequencies and buckling loads for thick plates. Some shortcomings of the classical plate theory are modified by a number of shear deformable plate theories the simplest of which is the first-order shear deformation theory (FSDT). The FSDT yields a constant value of transverse shear strain through the thickness of the plate and requires shear correction factors to account for the deviation of the actual transverse shear strain from the constant one. These shear correction factors are sensitive to the geometric parameters of plate, boundary conditions and loading conditions. To overcome the drawbacks of the FSDT, various higher-order plate theories have been proposed by assuming higher-order displacement fields. For instance, Reddy [1] developed a simple higher-order shear deformation plate theory by using third-order polynomial in the expansion of the displacement components through the thickness of the plate.

* Corresponding author. Tel.: +98 341 2111763; fax: +98 341 2120964.
E-mail address: saidi@mail.uk.ac.ir (A.R. Saidi).

0307-904X/$ - see front matter © 2010 Elsevier Inc. All rights reserved.
doi:10.1016/j.apm.2010.03.016

In recent years, a new class of materials known as functionally graded materials (FGM) has gained considerable attention as advanced structural materials because of their heat-shielding properties. Since in functionally graded plates, as opposed to isotropic plates, the condition of mid-plane symmetry no longer exists, the stretching and bending equations based on the higher-order shear deformation theory [1] are highly coupled so that the governing equations are five coupled partial differential equations in terms of five variables. It is not easy to solve them analytically except for some simple cases like axisymmetric circular or simply supported rectangular plates. Hence, the published articles concerning functionally graded (FG) plate problems based on the higher-order shear deformation theory (HSDT) are related to either the analytical solution for the mentioned simple cases or using numerical methods. Reddy [2] developed the Navier solutions and finite element models for simply supported functionally graded plates based on the third-order shear deformation theory (TSDT). Ma and Wang [3] employed the third-order shear deformation plate theory to solve the axisymmetric bending and buckling problems of functionally graded circular plates. They derived the relationships between the solutions of axisymmetric bending and buckling of FG plates based on the TSDT, and the solutions of the homogeneous plates obtained through the CPT. The critical buckling loads of FG simply supported rectangular thin plates were obtained by Javaheri and Eslami [4] using the CPT. Najafizadeh and Heydari [5,6] studied axisymmetric buckling analysis of thick functionally graded circular plates based on higher-order shear deformation plate theory, under uniform radial compression and different types of thermal loadings. They presented closed form solutions for the critical buckling load and temperature. Ferreira et al. [7] employed a meshless method to analyze the static deformation of a simply supported functionally graded plate using third-order shear deformation theory. Samsam Shariat and Eslami [8] presented the mechanical and thermal buckling analysis of thick functionally graded rectangular plate. They used higher-order shear deformation plate theory to obtain the closed form solution for the critical buckling load and temperature of a simply supported rectangular plate. It was assumed that the material properties vary linearly with respect to the thickness coordinate. They reported that the critical buckling mode may change as the aspect ratio increases. Zenkour [9] analyzed the static response of a simply supported functionally graded rectangular plate under a transverse uniform load by using a sinusoidal shear deformation theory. Axisymmetric bending and buckling of functionally graded circular plates was investigated by Saidi et al. [10] based on the unconstrained third-order shear deformation plate theory.

The bending problem of rectangular plates, with two opposite edges simply supported and different boundary conditions along the other edges, was successfully solved by Levy [11] in the late 19th century. Thereafter this method employed by many researchers to analyze static and dynamic analysis of plate structures [12–15]. Levy-type solutions for stresses analysis of laminated orthotropic composite plates developed by Reddy et al. [16] based on first-order shear deformation plate theory and state-space concept. Palardy and Palazotto [17] presented buckling loads and fundamental frequencies of laminated cross-ply plates using the Levy method. Chen and Liu [18] investigated thermal buckling of antisymmetric angle-ply laminated plates with Levy-type boundary conditions by an analytical technique in conjunction with the concept of state-space. Oktem and Chaudhuri [19] presented Levy-type analytical solution for the problem of deformation of finite-dimensional general cross-ply thick rectangular plates.

Reformulation of coupled governing equations by using the boundary layer function is a useful method for solving plate problems based on shear deformation theories. There are some studies in literature for solving the plate problems using this method. Nosier and Reddy [20,21] studied free vibration and buckling problems of a symmetric laminated plates with Levy boundary conditions based on Levinson and first-order theories by using boundary layer function. Jomehzadeh et al. [22] developed an analytical solution for bending of moderately thick FG sector plates in polar coordinates using the boundary layer function. Saidi and Jomehzadeh [23] reformulated the bending-stretching equations of FG rectangular plates with two opposite edges simply supported in terms of the boundary layer and transverse displacement functions based on first-order shear deformation theory. Using the boundary layer function, Atashipour et al. [24] presented a closed form solution for bending analysis of thick isotropic annular sector plates based on the third-order shear deformation theory. In recent research, Mohammadi et al. [25] investigated the buckling analysis of thin FG rectangular plate with various boundary conditions based on the classical plate theory.

Although some studies have been carried out for the static and dynamic analysis of plate by using boundary layer function based on shear deformation theories, no studies can be found for the buckling analysis of functionally graded rectangular plates or even homogeneous isotropic rectangular plates by using boundary layer function and Levy-type solution for different boundary condition based on higher-order shear deformation plate theory. In the present study, based on higher-order shear deformation plate theory, an analytical method for buckling analysis of functionally graded rectangular plates is investigated by using the boundary layer function. Introducing an analytical method, the governing stability equations of functionally graded plates are decoupled. Five coupled partial differential equations of FG plates are converted into two uncoupled equations in terms of transverse displacement and the boundary layer function. These equations are solved for the functionally graded rectangular plate with two opposite edges simply supported subjected to different types of in-plane loading. By imposing different boundary conditions along two other edges, the critical buckling loads are obtained for FG rectangular plate. Comparisons are investigated with the available data in literature for special case of simply supported thick plate, which show the high accuracy of the present formulations and procedures. Also, the present results are compared with those reported for thin FG plates based on CPT. Finally, the critical buckling loads are tabulated and shown for a FG plate with different boundary conditions and loading types, various powers of FGM and some thickness-side and aspect ratios. The presented results in this article can be used as benchmark.

2. Mechanical properties of FG rectangular plate

Consider a functionally graded rectangular plate which its mechanical properties vary smoothly and continuously along the thickness direction from one surface to the other. This is achieved by gradually varying the volume fraction of the constituent materials. FGMs are typically made from a mixture of ceramics and metal or a combination of different metals. It is considered that the FG rectangular plate is made of ceramic and metal. The effective material properties such as Young modulus E can be determined as (see e.g. [2–10])

$$E(z) = E_m + (E_c - E_m)\left(\frac{1}{2} - \frac{z}{h}\right)^n, \tag{1}$$

where the variable z is the thickness coordinate $(-h/2 \leqslant z \leqslant h/2)$, h is the thickness of the plate and n denotes the power of FGM which takes values greater than or equal to zero. Subscripts m and c refer to the metal and ceramic constituents, respectively. The variation of the composition of ceramic and metal is linear for $n = 1$. Also, the power of FGM equal to zero represents a full-ceramic plate. The variation of Poisson's ratio v is generally small and it is assumed to be a constant for convenience [2–6,8–10,22,23,25–27].

3. Equilibrium and stability equations based on the HSDT

The higher-order shear deformation plate theory of Reddy [1] accommodates a quadratic variation of the transverse shear strain across the thickness and the vanishing shear stresses on the top and bottom surfaces of the plate. This theory yields the following displacement field [1]

$$\begin{aligned} U_1(x,y,z) &= u(x,y) + z\psi_x(x,y) - \alpha z^3[\psi_x(x,y) + w_{,x}],\\ U_2(x,y,z) &= v(x,y) + z\psi_y(x,y) - \alpha z^3[\psi_y(x,y) + w_{,y}],\\ U_3(x,y,z) &= w(x,y), \end{aligned} \tag{2}$$

where u and v are the mid-plane displacements of the plate in the x and y directions, respectively, w is the transverse displacement and ψ_x and ψ_y are rotation functions of the middle surface in the x and y directions, respectively, and $\alpha = 4/(3h^2)$. Also, subscripts (,) denotes the differentiation with respect to the Cartesian coordinate. Note that unlike the FSDT, the higher-order plate theory requires no shear correction factors.

By consideration the Von-Karman hypothesis for non-linear relation of strain–displacement [28], the kinematic relations are obtained as follows:

$$\begin{aligned} \begin{pmatrix} \varepsilon_{xx} \\ \varepsilon_{yy} \\ \gamma_{xy} \end{pmatrix} &= \begin{pmatrix} \varepsilon^{(0)}_{xx} \\ \varepsilon^{(0)}_{yy} \\ \gamma^{(0)}_{xy} \end{pmatrix} + z\begin{pmatrix} \varepsilon^{(1)}_{xx} \\ \varepsilon^{(1)}_{yy} \\ \gamma^{(1)}_{xy} \end{pmatrix} + z^3\begin{pmatrix} \varepsilon^{(3)}_{xx} \\ \varepsilon^{(3)}_{yy} \\ \gamma^{(3)}_{xy} \end{pmatrix},\\ \begin{pmatrix} \gamma_{xz} \\ \gamma_{yz} \end{pmatrix} &= \begin{pmatrix} \gamma^{(0)}_{xz} \\ \gamma^{(0)}_{yz} \end{pmatrix} + z^2\begin{pmatrix} \gamma^{(2)}_{xz} \\ \gamma^{(2)}_{yz} \end{pmatrix}, \end{aligned} \tag{3}$$

where

$$\begin{aligned} &\begin{pmatrix} \varepsilon^{(0)}_{xx} \\ \varepsilon^{(0)}_{yy} \\ \gamma^{(0)}_{xy} \end{pmatrix} = \begin{pmatrix} u_{,x} + (w_{,x})^2/2 \\ v_{,y} + (w_{,y})^2/2 \\ u_{,y} + v_{,x} + w_{,x}w_{,y} \end{pmatrix}; \quad \begin{pmatrix} \varepsilon^{(1)}_{xx} \\ \varepsilon^{(1)}_{yy} \\ \gamma^{(1)}_{xy} \end{pmatrix} = \begin{pmatrix} \psi_{x,x} \\ \psi_{y,y} \\ \psi_{x,y} + \psi_{y,x} \end{pmatrix}; \quad \begin{pmatrix} \varepsilon^{(3)}_{xx} \\ \varepsilon^{(3)}_{yy} \\ \gamma^{(3)}_{xy} \end{pmatrix} = -\alpha\begin{pmatrix} \psi_{x,x} + w_{,xx} \\ \psi_{y,y} + w_{,yy} \\ \psi_{x,y} + \psi_{y,x} + 2w_{,xy} \end{pmatrix},\\ &\begin{pmatrix} \gamma^{(0)}_{xz} \\ \gamma^{(0)}_{yz} \end{pmatrix} = \begin{pmatrix} \psi_x + w_{,x} \\ \psi_y + w_{,y} \end{pmatrix}; \quad \begin{pmatrix} \gamma^{(2)}_{xz} \\ \gamma^{(2)}_{yz} \end{pmatrix} = -\beta\begin{pmatrix} \psi_x + w_{,x} \\ \psi_y + w_{,y} \end{pmatrix}; \quad \beta = 3\alpha = 4/h^2. \end{aligned} \tag{4}$$

Assuming the plane stress state, Hooke's law for a plate can be written as follows:

$$\begin{Bmatrix} \sigma_{xx} \\ \sigma_{yy} \\ \sigma_{xy} \\ \sigma_{xz} \\ \sigma_{yz} \end{Bmatrix} = \begin{bmatrix} Q_{11} & Q_{12} & 0 & 0 & 0 \\ Q_{12} & Q_{11} & 0 & 0 & 0 \\ 0 & 0 & Q_{22} & 0 & 0 \\ 0 & 0 & 0 & Q_{22} & 0 \\ 0 & 0 & 0 & 0 & Q_{22} \end{bmatrix}\begin{Bmatrix} \varepsilon_{xx} \\ \varepsilon_{yy} \\ \gamma_{xy} \\ \gamma_{xz} \\ \gamma_{yz} \end{Bmatrix}, \tag{5}$$

where

$$Q_{11} = \frac{E(z)}{(1-v^2)}, \quad Q_{12} = vQ_{11}, \quad Q_{22} = \frac{E(z)}{2(1+v)} \tag{6}$$

Using the principle of minimum total potential energy as [15]

$$\delta(U+V)=0, \tag{7}$$

where δ represents the variational symbol; U and V are the strain energy of the plate and the potential energy of external loads, respectively. Substituting the resulting strains into the principle of minimum total potential energy, the equilibrium equations can be obtained as follows:

$$\begin{aligned}
&\delta u: N_{xx,x}+N_{xy,y}=0,\\
&\delta v: N_{xy,x}+N_{yy,y}=0,\\
&\delta\psi_x: M_{xx,x}+M_{xy,y}-Q_x-\alpha(P_{xx,x}+P_{xy,y})+\beta R_x=0,\\
&\delta\psi_y: M_{xy,x}+M_{yy,y}-Q_y-\alpha(P_{xy,x}+P_{yy,y})+\beta R_y=0,\\
&\delta w: Q_{x,x}+Q_{y,y}+\alpha(P_{xx,xx}+2P_{xy,xy}+P_{yy,yy})-\beta(R_{x,x}+R_{y,y})+N_{xx}w_{,xx}+2N_{xy}w_{,xy}+N_{yy}w_{,yy}=0,
\end{aligned} \tag{8}$$

where N_i, M_i, P_i $(i=xx,yy,xy)$ are the resultant forces, moments, and higher-order moments, respectively, and Q_i, R_i $(i=x,y)$ are, respectively, the shear forces and higher-order shear forces which are all defined by the following expressions:

$$(N_i,M_i,P_i)=\int_{-h/2}^{h/2}(1,z,z^3)\sigma_i dz,\ (i=xx,yy,xy), \tag{9a}$$

$$(Q_i,R_i)=\int_{-h/2}^{h/2}(1,z^2)\sigma_{iz}dz,\ (i=x,y). \tag{9b}$$

By substituting Eq. (3) into Eq. (5) and the subsequent results into Eq. (9), the stress resultants are obtained in the matrix form as

$$\begin{Bmatrix} N_{xx}\\ N_{yy}\\ N_{xy}\\ M_{xx}\\ M_{yy}\\ M_{xy}\\ P_{xx}\\ P_{yy}\\ P_{xy}\end{Bmatrix}=\begin{bmatrix} A_{11} & A_{12} & 0 & B_{11} & B_{12} & 0 & -\alpha D_{11} & -\alpha D_{12} & 0\\ A_{12} & A_{11} & 0 & B_{12} & B_{11} & 0 & -\alpha D_{12} & -\alpha D_{11} & 0\\ 0 & 0 & A_{22} & 0 & 0 & B_{22} & 0 & 0 & -\alpha D_{22}\\ B_{11} & B_{12} & 0 & C_{11} & C_{12} & 0 & -\alpha F_{11} & -\alpha F_{12} & 0\\ B_{12} & B_{11} & 0 & C_{12} & C_{11} & 0 & -\alpha F_{12} & -\alpha F_{11} & 0\\ 0 & 0 & B_{22} & 0 & 0 & C_{22} & 0 & 0 & -\alpha F_{22}\\ D_{11} & D_{12} & 0 & F_{11} & F_{12} & 0 & -\alpha H_{11} & -\alpha H_{12} & 0\\ D_{12} & D_{11} & 0 & F_{12} & F_{11} & 0 & -\alpha H_{12} & -\alpha H_{11} & 0\\ 0 & 0 & D_{22} & 0 & 0 & F_{22} & 0 & 0 & -\alpha H_{22}\end{bmatrix}\begin{Bmatrix} u_{,x}+(w_{,x})^2/2\\ v_{,y}+(w_{,y})^2/2\\ u_{,y}+v_{,x}+w_{,x}w_{,y}\\ \psi_{x,x}\\ \psi_{y,y}\\ \psi_{x,y}+\psi_{y,x}\\ \psi_{x,x}+w_{,xx}\\ \psi_{y,y}+w_{,yy}\\ \psi_{x,y}+\psi_{y,x}+2w_{,xy}\end{Bmatrix}, \tag{10a}$$

$$\begin{Bmatrix} Q_x\\ Q_y\\ R_x\\ R_y\end{Bmatrix}=\begin{bmatrix} A_{22}-\beta C_{22} & 0\\ 0 & A_{22}-\beta C_{22}\\ C_{22}-\beta F_{22} & 0\\ 0 & C_{22}-\beta F_{22}\end{bmatrix}\begin{Bmatrix}\psi_x+w_{,x}\\ \psi_y+w_{,y}\end{Bmatrix}, \tag{10b}$$

where $(A_{ij},B_{ij},C_{ij},D_{ij},F_{ij},H_{ij})$ are the plate stiffness coefficients defined by

$$(A_{ij},B_{ij},C_{ij},D_{ij},F_{ij},H_{ij})=\int_{-h/2}^{h/2}(1,z,z^2,z^3,z^4,z^6)Q_{ij}dz,\quad i,j=1,2. \tag{11}$$

Focusing on the relations (6) and (11), it is observed that

$$(A_{12},B_{12},C_{12},D_{12},F_{12},H_{12})=(A_{11},B_{11},C_{11},D_{11},F_{11},H_{11})-2(A_{22},B_{22},C_{22},D_{22},F_{22},H_{22}). \tag{12}$$

In order to study the buckling behavior of the plate and obtain the stability equations, the adjacent equilibrium criterion is used [28]. Assume that the equilibrium state of a plate under mechanical loads is defined in terms of the displacement components u^0, v^0, w^0, ψ_x^0 and ψ_y^0. Due to forces and/or moments, a neighboring stable state could be created. The displacement components of a neighboring state differ by u^1, v^1, w^1, ψ_x^1 and ψ_y^1 with respect to the equilibrium position. Thus, the total displacements of a neighboring state are

$$\begin{aligned}
&u\to u^0+u^1;\quad v\to v^0+v^1;\quad w\to w^0+w^1,\\
&\psi_x\to\psi_x^0+\psi_x^1;\quad \psi_y\to\psi_y^0+\psi_y^1.
\end{aligned} \tag{13}$$

Upon substituting the relations (13) in Eq. (10), the expressions for stress resultants related to the equilibrium and neighboring states are obtained. Equivalently, the stress resultants can be written as

$$
\begin{aligned}
&N_{xx} = N^0_{xx} + N^1_{xx}; \quad N_{yy} = N^0_{yy} + N^1_{yy}; \quad N_{xy} = N^0_{xy} + N^1_{xy},\\
&M_{xx} = M^0_{xx} + M^1_{xx}; \quad M_{yy} = M^0_{yy} + M^1_{yy}; \quad M_{xy} = M^0_{xy} + M^1_{xy},\\
&P_{xx} = P^0_{xx} + P^1_{xx}; \quad P_{yy} = P^0_{yy} + P^1_{yy}; \quad P_{xy} = P^0_{xy} + P^1_{xy},\\
&R_x = R^0_x + R^1_x; \quad R_y = R^0_y + R^1_y; \quad Q_x = Q^0_x + Q^1_x; \quad Q_y = Q^0_y + Q^1_y,
\end{aligned}
\tag{14}
$$

where the terms with subscripts 0 related to the equilibrium state and the terms with subscripts 1 are linear parts of the stress resultants increments corresponding to the neighboring state.

The stability equations may be obtained by substituting Eqs. (13) and (14) into Eq. (8). Upon substitution, the terms in the resulting equations with superscript 0 satisfy the equilibrium condition and therefore omitted from the equations. Also, the non-linear terms with superscript 1 are ignored because they are small compared to the linear terms [8]. The remaining terms form the stability equations of functionally graded rectangular plate as

$$
\begin{aligned}
&N^1_{xx,x} + N^1_{xy,y} = 0,\\
&N^1_{xy,x} + N^1_{yy,y} = 0,\\
&M^1_{xx,x} + M^1_{xy,y} - Q^1_x - \alpha(P^1_{xx,x} + P^1_{xy,y}) + \beta R^1_x = 0,\\
&M^1_{xy,x} + M^1_{yy,y} - Q^1_y - \alpha(P^1_{xy,x} + P^1_{yy,y}) + \beta R^1_y = 0,\\
&Q^1_{x,x} + Q^1_{y,y} + \alpha(P^1_{xx,xx} + 2P^1_{xy,xy} + P^1_{yy,yy}) - \beta(R^1_{x,x} + R^1_{y,y}) + N^0_{xx}w^1_{,xx} + 2N^0_{xy}w^1_{,xy} + N^0_{yy}w^1_{,yy} = 0.
\end{aligned}
\tag{15}
$$

These equations are five coupled stability equations of the plate subjected to the in-plane edge loading. Also, the parameters N^0_i $(i = xx, yy, xy)$ can be replaced by the pre-buckling forces obtained from equilibrium conditions.

4. Decoupling governing stability equations

The governing stability equations of functionally graded plate are obtained by substituting the equivalent neighboring form of Eq. (10) into stability Eq. (15) as

$$
\begin{aligned}
&A_{11}u^1_{,xx} + A_{12}v^1_{,yx} + B_{11}\psi^1_{x,xx} + B_{12}\psi^1_{y,yx} - \alpha D_{11}\left(\psi^1_{x,x} + w^1_{,xx}\right)_{,x} - \alpha D_{12}\left(\psi^1_{y,y} + w^1_{,yy}\right)_{,x} + A_{22}\left(u^1_{,y} + v^1_{,x}\right)_{,y}\\
&\quad + B_{22}\left(\psi^1_{x,y} + \psi^1_{y,x}\right)_{,y} - \alpha D_{22}\left(\psi^1_{x,y} + \psi^1_{y,x} + 2w^1_{,xy}\right)_{,y} = 0,
\end{aligned}
\tag{16a}
$$

$$
\begin{aligned}
&A_{11}v^1_{,yy} + A_{12}u^1_{,xy} + B_{11}\psi^1_{y,yy} + B_{12}\psi^1_{x,xy} - \alpha D_{11}\left(\psi^1_{y,y} + w^1_{,yy}\right)_{,y} - \alpha D_{12}\left(\psi^1_{x,x} + w^1_{,xx}\right)_{,y} + A_{22}\left(u^1_{,y} + v^1_{,x}\right)_{,x}\\
&\quad + B_{22}\left(\psi^1_{x,y} + \psi^1_{y,x}\right)_{,x} - \alpha D_{22}\left(\psi^1_{x,y} + \psi^1_{y,x} + 2w^1_{,xy}\right)_{,x} = 0,
\end{aligned}
\tag{16b}
$$

$$
\begin{aligned}
&(B_{11} - \alpha D_{11})u^1_{,xx} + (B_{12} - \alpha D_{12})v^1_{,yx} + (C_{11} - \alpha F_{11})\psi^1_{x,xx} + (C_{12} - \alpha F_{12})\psi^1_{y,yx} - \alpha(F_{11} - \alpha H_{11})\left(\psi^1_{x,x} + w^1_{,xx}\right)_{,x}\\
&\quad - \alpha(F_{12} - \alpha H_{12})\left(\psi^1_{y,y} + w^1_{,yy}\right)_{,x} + (B_{22} - \alpha D_{22})\left(u^1_{,y} + v^1_{,x}\right)_{,y} + (C_{22} - \alpha F_{22})\left(\psi^1_{x,y} + \psi^1_{y,x}\right)_{,y}\\
&\quad - \alpha(F_{22} - \alpha H_{22})\left(\psi^1_{x,y} + \psi^1_{y,x} + 2w^1_{,xy}\right)_{,y} - (A_{22} - 2\beta C_{22} + \beta^2 F_{22})\left(\psi^1_{x} + w^1_{,x}\right) = 0,
\end{aligned}
\tag{16c}
$$

$$
\begin{aligned}
&(B_{11} - \alpha D_{11})v^1_{,yy} + (B_{12} - \alpha D_{12})u^1_{,xy} + (C_{11} - \alpha F_{11})\psi^1_{y,yy} + (C_{12} - \alpha F_{12})\psi^1_{x,xy} - \alpha(F_{11} - \alpha H_{11})\left(\psi^1_{y,y} + w^1_{,yy}\right)_{,y}\\
&\quad - \alpha(F_{12} - \alpha H_{12})\left(\psi^1_{x,x} + w^1_{,xx}\right)_{,y} + (B_{22} - \alpha D_{22})\left(u^1_{,y} + v^1_{,x}\right)_{,x} + (C_{22} - \alpha F_{22})\left(\psi^1_{x,y} + \psi^1_{y,x}\right)_{,x}\\
&\quad - \alpha(F_{22} - \alpha H_{22})\left(\psi^1_{x,y} + \psi^1_{y,x} + 2w^1_{,xy}\right)_{,x} - (A_{22} - 2\beta C_{22} + \beta^2 F_{22})\left(\psi^1_{y} + w^1_{,y}\right) = 0,
\end{aligned}
\tag{16d}
$$

$$
\begin{aligned}
&\alpha\Big\{D_{11}\left(u^1_{,xxx} + v^1_{,yyy}\right) + D_{12}\left(u^1_{,xyy} + v^1_{,yxx}\right) + F_{11}\left(\psi^1_{x,xxx} + \psi^1_{y,yyy}\right) + F_{12}\left(\psi^1_{x,xyy} + \psi^1_{y,yxx}\right)\\
&\quad - \alpha H_{11}\left[\left(\psi^1_{x,x} + w^1_{,xx}\right)_{,xx} + \left(\psi^1_{y,y} + w^1_{,yy}\right)_{,yy}\right] - \alpha H_{12}\left[\left(\psi^1_{y,y} + w^1_{,yy}\right)_{,xx} + \left(\psi^1_{x,x} + w^1_{,xx}\right)_{,yy}\right]\\
&\quad + 2D_{22}\left(u^1_{,y} + v^1_{,x}\right)_{,xy} + 2F_{22}\left(\psi^1_{x,y} + \psi^1_{y,x}\right)_{,xy} - 2\alpha H_{22}\left(\psi^1_{x,y} + \psi^1_{y,x} + 2w^1_{,xy}\right)_{,xy}\Big\}\\
&\quad + (A_{22} - 2\beta C_{22} + \beta^2 F_{22})\left[\left(\psi^1_{x} + w^1_{,x}\right)_{,x} + \left(\psi^1_{y} + w^1_{,y}\right)_{,y}\right] + N^0_{xx}w^1_{,xx} + 2N^0_{xy}w^1_{,xy} + N^0_{yy}w^1_{,yy} = 0.
\end{aligned}
\tag{16e}
$$

Eq. (16) are five highly coupled equations in terms of neighboring displacement components.

For solving such coupled equations, it is convenient to find a method for decoupling them. By using relation (12) and introducing four new analytical functions, the governing stability Eq. (16) are simplified as follows:

$$A_{11}\varphi_{1,x} + A_{22}\varphi_{2,y} + B_1\varphi_{3,x} + B_2\varphi_{4,y} - \alpha D_{11}\nabla^2 w^1_{,x} = 0, \tag{17a}$$
$$A_{11}\varphi_{1,y} - A_{22}\varphi_{2,x} + B_1\varphi_{3,y} - B_2\varphi_{4,x} - \alpha D_{11}\nabla^2 w^1_{,y} = 0, \tag{17b}$$
$$B_1\varphi_{1,x} + B_2\varphi_{2,y} + C_1\varphi_{3,x} + C_2\varphi_{4,y} - A_2(\psi^1_x + w^1_{,x}) - H_1\nabla^2 w^1_{,x} = 0, \tag{17c}$$
$$B_1\varphi_{1,y} - B_2\varphi_{2,x} + C_1\varphi_{3,y} - C_2\varphi_{4,x} - A_2(\psi^1_y + w^1_{,y}) - H_1\nabla^2 w^1_{,y} = 0, \tag{17d}$$
$$\alpha D_{11}\nabla^2\varphi_1 + H_1\nabla^2\varphi_3 - \alpha^2 H_{11}\nabla^4 w^1 + A_2(\nabla^2 w^1 + \varphi_3) + N^0_{xx}w^1_{,xx} + 2N^0_{xy}w^1_{,xy} + N^0_{yy}w^1_{,yy} = 0, \tag{17e}$$

where ∇^2 is two-dimensional Laplacian operator and the functions φ_i $(i = 1, 2, 3, 4)$ are defined as

$$\begin{Bmatrix} \varphi_1 \\ \varphi_2 \\ \varphi_3 \\ \varphi_4 \end{Bmatrix} = \begin{Bmatrix} u^1_{,x} + v^1_{,y} \\ u^1_{,y} - v^1_{,x} \\ \psi^1_{x,x} + \psi^1_{y,y} \\ \psi^1_{x,y} - \psi^1_{y,x} \end{Bmatrix}. \tag{18}$$

The constant coefficients in Eq. (17) are also defined as

$$\begin{aligned} &B_1 = B_{11} - \alpha D_{11}; \quad C_1 = C_{11} - 2\alpha F_{11} + \alpha^2 H_{11}, \\ &B_2 = B_{22} - \alpha D_{22}; \quad C_2 = C_{22} - 2\alpha F_{22} + \alpha^2 H_{22}, \\ &H_1 = \alpha F_{11} - \alpha^2 H_{11}; \quad A_2 = A_{22} - 2\beta C_{22} + \beta^2 F_{22}. \end{aligned} \tag{19}$$

Multiplying Eqs. (17a) and (17b) by B_1/A_{11} and considering $B_2 = B_1A_{22}/A_{11}$, yields

$$B_1\varphi_{1,x} + B_2\varphi_{2,y} = -\frac{B_1^2}{A_{11}}\varphi_{3,x} - \frac{B_1B_2}{A_{11}}\varphi_{4,y} + \frac{\alpha D_{11}B_1}{A_{11}}\nabla^2 w^1_{,x}, \tag{20a}$$
$$B_1\varphi_{1,y} - B_2\varphi_{2,x} = -\frac{B_1^2}{A_{11}}\varphi_{3,y} + \frac{B_1B_2}{A_{11}}\varphi_{4,x} + \frac{\alpha D_{11}B_1}{A_{11}}\nabla^2 w^1_{,y}. \tag{20b}$$

Also, adding the differentiation of Eq. (20a) with respect to x and Eq. (20b) with respect to y, yields

$$\nabla^2\varphi_1 = -\frac{B_1}{A_{11}}\nabla^2\varphi_3 + \frac{\alpha D_{11}}{A_{11}}\nabla^4 w^1. \tag{21}$$

Similarly, subtraction of the differentiation of Eq. (20a) with respect to y and Eq. (20b) with respect to x, it is concluded that

$$\nabla^2\varphi_2 = -\frac{B_1}{A_{11}}\nabla^2\varphi_4. \tag{22}$$

Using Eqs. (20) and (21), the last three equation of Eq. (17) can be expressed as

$$\widehat{C}\varphi_{3,x} + \widehat{B}\varphi_{4,y} - \hat{A}(\psi_x + w^1_{,x}) - \hat{H}\nabla^2 w^1_{,x} = 0, \tag{23a}$$
$$\widehat{C}\varphi_{3,y} - \widehat{B}\varphi_{4,x} - \hat{A}(\psi_y + w^1_{,y}) - \hat{H}\nabla^2 w^1_{,y} = 0, \tag{23b}$$
$$\hat{H}\nabla^2\varphi_3 - \hat{F}\nabla^4 w^1 + \hat{A}(\nabla^2 w^1 + \varphi_3) + N^0_{xx}w^1_{,xx} + 2N^0_{xy}w^1_{,xy} + N^0_{yy}w^1_{,yy} = 0, \tag{23c}$$

where

$$\begin{aligned} &\widehat{C} = C_1 - \tfrac{B_1^2}{A_{11}}; \quad \widehat{B} = C_2 - \tfrac{B_1B_2}{A_{11}}; \quad \hat{A} = A_2, \\ &\widehat{H} = H_1 - \tfrac{\alpha D_{11}B_1}{A_{11}}; \quad \widehat{F} = \alpha^2\left(H_{11} - \tfrac{D_{11}^2}{A_{11}}\right). \end{aligned} \tag{24}$$

It can be seen from Eq. (23) that the terms containing the mid-plane displacements (u and v) are uncoupled from the rotation functions (ψ_x and ψ_y) and the transverse displacement (w).

By using some algebraic operations, three extensively coupled Eq. (23) may be also converted into two uncoupled equations in the form

$$\widehat{B}\nabla^2\varphi_4 - \hat{A}\varphi_4 = 0, \tag{25a}$$
$$\overline{C}\nabla^6 w^1 - \overline{D}\nabla^4 w^1 = \frac{\widehat{C}}{\widehat{A}}\nabla^2\left(N^0_{xx}w^1_{,xx} + 2N^0_{xy}w^1_{,xy} + N^0_{yy}w^1_{,yy}\right) - \left(N^0_{xx}w^1_{,xx} + 2N^0_{xy}w^1_{,xy} + N^0_{yy}w^1_{,yy}\right), \tag{25b}$$

where the parameters $\overline{C}$, $\overline{D}$ are defined as

$$\overline{C}=\frac{\widehat{F}\widehat{C}-\widehat{H}^2}{\widehat{A}};\quad \overline{D}=C_{11}-\frac{B_{11}^2}{A_{11}}. \tag{26}$$

Eq. (25a) is known as the edge-zone (or boundary layer) equation of the plate, and the function φ_4 is referred to the boundary layer function. Also, Eq. (25b) is called the interior equation of the plate.

Also, it can be seen that the rotation functions ψ_x and ψ_y can be expressed in terms of w and φ_4 as

$$\psi_x^1=\left(\frac{\widehat{C}\overline{C}}{\widehat{A}(\widehat{C}+\widehat{H})}\nabla^4 w^1-\frac{(\widehat{C}+\widehat{H})}{\widehat{A}}\nabla^2 w^1-w^1-\frac{\widehat{C}^2}{\widehat{A}^2(\widehat{C}+\widehat{H})}\left(N_{xx}^0 w_{,xx}^1+2N_{xy}^0 w_{,xy}^1+N_{yy}^0 w_{,yy}^1\right)\right)_{,x}+\frac{\widehat{B}}{\widehat{A}}\varphi_{4,y}, \tag{27a}$$

$$\psi_y^1=\left(\frac{\widehat{C}\overline{C}}{\widehat{A}(\widehat{C}+\widehat{H})}\nabla^4 w^1-\frac{(\widehat{C}+\widehat{H})}{\widehat{A}}\nabla^2 w^1-w^1-\frac{\widehat{C}^2}{\widehat{A}^2(\widehat{C}+\widehat{H})}\left(N_{xx}^0 w_{,xx}^1+2N_{xy}^0 w_{,xy}^1+N_{yy}^0 w_{,yy}^1\right)\right)_{,y}-\frac{\widehat{B}}{\widehat{A}}\varphi_{4,x}. \tag{27b}$$

Details of deriving Eqs. (25) and (27) are given in Appendix A.

Considering the definition of functions φ_i $(i=1,2,3,4)$ in relations (18), it is easy to show that the Eqs. (21) and (22) can be satisfied by assuming the in-plane displacement as follows:

$$\begin{aligned} u^1&=-\frac{B_{11}}{A_{11}}\psi_x^1+\frac{\alpha D_{11}}{A_{11}}\left(\psi_x^1+w_{,x}^1\right),\\ v^1&=-\frac{B_{11}}{A_{11}}\psi_y^1+\frac{\alpha D_{11}}{A_{11}}\left(\psi_y^1+w_{,y}^1\right). \end{aligned} \tag{28}$$

It can be shown that relations (28) satisfy not only Eqs. (21) and (22), but the boundary conditions of the plate. Note that for homogeneous isotropic plates the parameters B_{ij} and D_{ij} are zero which in this case the in-plane displacements vanish as expected.

5. Buckling analysis

5.1. In-plane loading conditions

Consider a rectangular plate with length a and width b which is subjected to an in-plane loading in two directions, as shown in Fig. 1. Therefore, the pre-buckling forces can be obtained using the equilibrium conditions as

$$N_{xx}^0=-P_1;\quad N_{yy}^0=-P_2;\quad N_{xy}^0=0, \tag{29}$$

where P_1 and P_2 are the forces per unit length. Substituting relations (29) into Eq. (25b) yields

$$\overline{C}\nabla^6 w^1-\overline{D}\nabla^4 w^1=-\frac{\widehat{C}}{\widehat{A}}\nabla^2\left(P_1 w_{,xx}^1+P_2 w_{,yy}^1\right)+\left(P_1 w_{,xx}^1+P_2 w_{,yy}^1\right). \tag{30}$$

There are two independent load parameters P_1 and P_2 in Eq. (30). This equation can be simplified to a single parameter equation by letting $P_2=RP_1$, where R is a non-dimensional load parameter which indicates the loading conditions. The plate is subjected to biaxial compression, when R is positive and it is under uniaxial compression along the x axis, when R is equal to zero. Also, negative values of R signify tensile loading in the y direction while the plate is under compressive loading along the x direction.

5.2. Levy-type solution

The FG rectangular plate is assumed to be simply supported along two opposite edges in y direction. Then, the following series solution is chosen for the transverse displacement w^1 and the function φ_4 as [20–24]

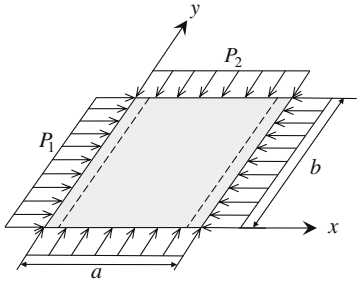

Fig. 1. The rectangular plate subjected to in-plane loading.

$$w^1(x,y)=\sum_{m=1}^{\infty} f(y)\sin(\lambda_m x), \tag{31a}$$

$$\varphi_4(x,y)=\sum_{m=1}^{\infty} g(y)\cos(\lambda_m x), \tag{31b}$$

where λ_m denotes $m\pi/a$ and m is the number of half-waves in the x direction of buckling mode shape and the function $f(y)$ represents the buckling mode shape along the y axis. Also, It can be seen that Eq. (31) exactly satisfy the simply supported boundary conditions at $x=0$ and $x=a$ [1]. Upon substitution of Eq. (31a) into Eq. (30) and simplifying the result, the following ordinary differential equation can be obtained:

$$f^{(6)}(y)+S_1 f^{(4)}(y)+S_2 f^{(2)}(y)+S_3 f(y)=0, \tag{32}$$

where the parameters S_i $(i=1,2,3)$ are

$$\begin{aligned} S_1&=-\left(3\lambda_m^2+\frac{\overline{D}}{\overline{C}}-\frac{\widehat{C}RP_1}{\widehat{A}\overline{C}}\right),\\ S_2&=3\lambda_m^4+\frac{2\lambda_m^2\overline{D}}{\overline{C}}-\frac{P_1}{\overline{C}}\left(\frac{\lambda_m^2\widehat{C}}{\widehat{A}}+R\left(1+\frac{\lambda_m^2\widehat{C}}{\widehat{A}}\right)\right),\\ S_3&=-\lambda_m^2\left(\lambda_m^4+\frac{\lambda_m^2\overline{D}}{\overline{C}}-\frac{P_1}{\overline{C}}\left(1+\frac{\lambda_m^2\widehat{C}}{\widehat{A}}\right)\right). \end{aligned} \tag{33}$$

The solution of this ordinary differential equation can be expressed as

$$f(y)=\exp(ky). \tag{34}$$

Substituting the above equation into Eq. (32), gives the following characteristic equation:

$$k^6+S_1k^4+S_2k^2+S_3=0. \tag{35}$$

By change of the variable $(t=k^2)$, Eq. (35) can be rewritten as

$$t^3+S_1t^2+S_2t+S_3=0. \tag{36}$$

The characteristic Eq. (36) has the three roots t_i $(i=1,2,3)$ which by considering relation $(t=k^2),\ k_i=\pm\sqrt{t_i}$ $(i=1,2,3)$ are roots of the Eq. (35). For solving the characteristic Eq. (36), three new parameters $p,\ q$ and G are introduced as

$$\begin{aligned} p&=\frac{3S_2-S_1^2}{9},\\ q&=\frac{9S_1S_2-27S_3-2S_1^3}{54},\\ G&=p^3+q^2. \end{aligned} \tag{37}$$

By investigating, it is observed that the three roots of Eq. (36) may be real or complex quantities depending on the sign of G (positive, zero or negative). Consequently the solution of ordinary differential Eq. (32) may be different for various sign of G. Since the sign of G depending on the unknown buckling load, it is necessary to investigate of all the possible cases. Three general cases can happen as follows:

Case 1: $G>0$

In this case the general solution of Eq. (32) involves the hyperbolic and trigonometric functions with six unknown constants of integration as follows:

$$\begin{aligned} f(y)=&c_1\cosh(k_1y)+c_2\sinh(k_1y)+c_3\cosh(k_2y)\cos(k_3y)+c_4\cosh(k_2y)\sin(k_3y)+c_5\sinh(k_2y)\cos(k_3y)\\ &+c_6\sinh(k_2y)\sin(k_3y), \end{aligned} \tag{38}$$

where $k_i=\sqrt{t_i}$ $(i=1,2,3)$, and the parameters t_i $(i=1,2,3)$ are defined as

$$\begin{aligned} t_1&=V_1,\\ t_2&=\frac{1}{2}\left(\sqrt{V_2^2+V_3^2}+V_2\right),\\ t_3&=\frac{1}{2}\left(\sqrt{V_2^2+V_3^2}-V_2\right), \end{aligned} \tag{39}$$

and

$$V_1 = L_1 + L_2 - \frac{S_1}{3}; \quad V_2 = -\left(\frac{L_1 + L_2}{2} + \frac{S_1}{3}\right); \quad V_3 = \frac{\sqrt{3}}{2}(L_1 - L_2),$$
$$L_1 = \sqrt[3]{q + \sqrt{G}}; \quad L_2 = \sqrt[3]{q - \sqrt{G}}. \tag{40}$$

Case 2: $G = 0$

The general solution of Eq. (32) in this case can be expressed as

$$f(y) = c_1 \cosh(k_1 y) + c_2 \sinh(k_1 y) + c_3 \cosh(k_2 y) + c_4 \sinh(k_2 y) + y(c_5 \cosh(k_2 y) + c_6 \sinh(k_2 y)), \tag{41}$$

where $k_i = \sqrt{t_i}$ $(i = 1, 2)$, and the parameters t_i $(i = 1, 2)$ are

$$t_1 = 2L_1 - \frac{S_1}{3},$$
$$t_2 = -\left(L_1 + \frac{S_1}{3}\right), \tag{42}$$

and

$$L_1 = \sqrt[3]{q + \sqrt{G}}; \quad L_2 = \sqrt[3]{q - \sqrt{G}}. \tag{43}$$

Case 3: $G < 0$

The general solutions of Eq. (32) in this case may be written as

$$f(y) = c_1 \cosh(k_1 y) + c_2 \sinh(k_1 y) + c_3 \cosh(k_2 y) + c_4 \sinh(k_2 y) + c_5 \cosh(k_3 y) + c_6 \sinh(k_3 y), \tag{44}$$

where $k_i = \sqrt{t_i}$ $(i = 1, 2, 3)$, and the parameters t_i $(i = 1, 2, 3)$ are defined as

$$t_1 = -\frac{S_1}{3} + 2\sqrt{-p}\cos\left(\frac{\theta}{3}\right),$$
$$t_2 = -\frac{S_1}{3} + 2\sqrt{-p}\cos\left(\frac{\theta + 2\pi}{3}\right), \quad \theta = \tan^{-1}\left(\frac{\sqrt{-G}}{q}\right), \tag{45}$$
$$t_3 = -\frac{S_1}{3} + 2\sqrt{-p}\cos\left(\frac{\theta + 4\pi}{3}\right).$$

It should be noted that in the Eqs. (38), (41) and (44), if $t_i < 0$ $(i = 1, 2, 3)$, let $\hat{k}_i = \sqrt{-t_i}$, then the hyperbolic functions $\cosh(k_i y)$ and $\sinh(k_i y)$ in the related equation are replaced with trigonometric functions $\cos(\hat{k}_i y)$ and $\sin(\hat{k}_i y)$.

In order to solve Eq. (25a), substituting the proposed series solution (31b) into Eq. (25a) yields one ordinary differential equation, which its general solution is given by

$$g(y) = c_7 \sinh(\mu y) + c_8 \cosh(\mu y), \tag{46}$$

where

$$\mu = \sqrt{\lambda_m^2 + \widehat{A}/\widehat{B}}. \tag{47}$$

Finally, upon substitution of Eq. (31) into Eq. (27), the general solution of rotation functions ψ_x and ψ_y can be also obtained.

5.3. Critical buckling load

As mentioned before, it is assumed that the FG plate is simply supported along two opposite edges in y direction. Therefore, the various boundary conditions (e.g. Clamped, Simply supported and Free) at two other edges of the rectangular plate ($y = 0$ and $y = b$) which are obtained from the principle of minimum total potential energy should be satisfied as follows:

$$\begin{aligned}
&\text{Clamped}: \ w^1 = w^1_{,y} = \psi^1_x = \psi^1_y = 0,\\
&\text{Simply Supported}: \ w^1 = \psi^1_x = M^1_{yy} = P^1_{yy} = 0,\\
&\text{Free}: \ M^1_{yy} = P^1_{yy} = M^1_{xy} - \alpha P^1_{xy} = \left(Q^1_y - \beta R^1_y\right) + \alpha\left(2P^1_{xy,x} + P^1_{yy,y}\right) + N^0_{yy} w^1_{,y} = 0.
\end{aligned} \tag{48}$$

By imposing different boundary conditions at two edges of the rectangular plate in direction x ($y = 0$ and $y = b$) a set of homogenous algebraic equations in terms of coefficients and buckling load P_1 for each longitudinal half-wave number (m) is obtained. To obtain a non-trivial solution of the system, the determinant of the eight order coefficient matrix is set equal to zero for the buckling loads which results the characteristic equation. Solving this equation, the buckling loads of the FG plate are evaluated. The lowest value among all these P_1 corresponds to the critical buckling load (P_{1cr}).

Through the text, the letter (S) indicates that the edge is simply supported, letter (C) means that the edge is clamped and letter (F) shows the free edge.

6. Comparative studies

In order to validate the accuracy of the present formulations and comparison the higher-order shear deformation theory with the classical plate theory, the critical buckling loads are compared with those available in the literature. Table 1 exhibits the comparison of the critical buckling loads obtained by the present analysis with respective values obtained by Samsam Shariat and Eslami [8] based on the HSDT, and Javaheri and Eslami [4] based on the CPT, for all edges simply supported FG plate. From Table 1, it is seen that there is an excellent agreement between the results obtained based on higher-order shear deformation plate theory, confirming the accuracy of the present solution. Also, it is concluded that the higher-order shear deformation theory accurately predicts the behavior of functionally graded plates, whereas the classical plate theory overestimates the critical buckling loads. Moreover, a comparative study has been performed in Table 2 for comparing the critical buckling loads obtained from the present solution with those reported by Mohammadi et al. [25] based on the classical plate theory. The comparison has been investigated for thin functionally graded rectangular plates with different boundary conditions and loading conditions and some power of FGM. From Table 2, it can be seen that for a thin plate ($h/b = 0.01$) the results are in good agreement, although, the classical plate theory slightly overestimates the critical buckling load.

Table 1
Comparison of the critical buckling loads (MN) for a simply supported functionally graded plate subjected to different loads versus the relative thickness ($a/b = 0.5$).

R		$b/h = 10$	$b/h = 20$	$b/h = 40$	$b/h = 60$	$b/h = 80$	$b/h = 100$
0	Ref. [4]	267.48	33.435	4.1794	1.2383	0.5224	0.2675
	Ref. [8]	239.15	32.472	4.1486	1.2343	0.5215	0.2672
	Present study	239.148	32.4721	4.14863	1.23427	0.52149	0.26725
1	Ref. [4]	213.99	26.748	3.4353	0.9907	0.4179	0.2140
	Ref. [8]	191.32	25.978	3.3189	0.9879	0.4172	0.2137
	Present study	191.319	25.9778	3.31890	0.98787	0.41716	0.21371
−1	Ref. [4]	356.64	44.580	5.5725	1.6511	0.6966	0.3566
	Ref. [8]	318.86	43.296	5.5315	1.6457	0.6953	0.3562
	Present study	318.856	43.2961	5.53153	1.64568	0.69528	0.35622

Table 2
Comparison of the critical buckling loads P_1 (MN/m) for a functionally graded rectangular plate with different boundary conditions ($h/b = 0.01$, $a/b = 1$).

R	n	Boundary condition					
			SCSC	*SSSC*	*SSSS*	*SCSF*	*SSSF*	*SFSF*
0	0	CPT[25]	2.64155[a]	1.97146	1.37379	0.56755	0.48137	0.32707
		HSDT	2.63583[a]	1.96946	1.373016	0.566082	0.480587	0.32379
	1	CPT[25]	1.31666[a]	0.98266	0.68475	0.28289	0.23994	0.16302
		HSDT	1.314254[a]	0.981818	0.684428	0.2822195	0.239282	0.162901
	2	CPT[25]	1.02741[a]	0.76678	0.53432	0.220744	0.18723	0.12721
		HSDT	1.025398[a]	0.766082	0.534053	0.220295	0.186948	0.127110
1	0	CPT[25]	1.31537	0.91450	0.68689	0.39275	0.36238	0.32016
		HSDT	1.313561	0.913696	0.686508	0.391107	0.361248	0.319712
	1	CPT[25]	0.65563	0.45582	0.34238	0.19576	0.18063	0.17119
		HSDT	0.654874	0.455486	0.342214	0.195017	0.180112	0.169379
	2	CPT[25]	0.511603	0.35569	0.26716	0.15276	0.14095	0.12452
		HSDT	0.510966	0.355405	0.267026	0.152152	0.140528	0.123360
−1	0	CPT[25]	3.70509[a]	3.22520[a]	2.86206[a]	0.85305	0.66578	0.33042
		HSDT	3.695187[a]	3.218978[a]	2.860035[a]	0.851958	0.665116	0.330109
	1	CPT[25]	1.84677[a]	1.60757[a]	1.42657[a]	0.42520	0.33185	0.16469
		HSDT	1.842606[a]	1.604957[a]	1.424877[a]	0.423336	0.3312753	0.164202
	2	CPT[25]	1.44106[a]	1.25442[a]	1.11318[a]	0.33179	0.25895	0.12851
		HSDT	1.43758[a]	1.25222[a]	1.111760[a]	0.330219	0.258332	0.128338

[a] Indicates the higher modes of buckling.

7. Results and discussion

After verifying the merit and accuracy of the present solutions, in order to obtain the following new results, it is assumed that the functionally graded plate is made of a mixture of Aluminum ($E_m = 70$ Gpa) and Silicon Carbide ($E_c = 420$ Gpa). The Poisson's ratio of the plate is assumed to be constant through the thickness and equal to 0.3. In Fig. 2, the critical buckling load for a FG plate with symmetric boundary conditions has been plotted versus the power of FGM. The FG plate is subjected to biaxial compression and tension along x and y directions, respectively. It can be seen that the critical buckling load decreases as the power of FGM increases. This is due to the fact that increasing the power of FGM increases the volume fraction of metal. Also, the critical buckling loads for homogeneous plates (e.g. full-ceramic plates) are considerably higher than those for the functionally graded plates ($n > 0$) and the variation of critical buckling load is noticeable when the power of FGM is small. Furthermore, the critical buckling mode shapes for three considered boundary conditions have a single half-wave in x

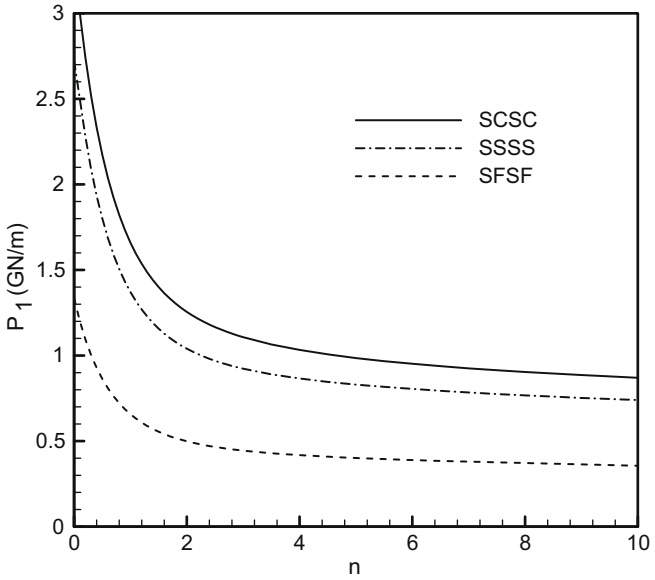

Fig. 2. The critical buckling load for a FG plate with symmetric boundary conditions versus the power of FGM ($a/b = 0.5,\ h/b = 0.1,\ R = -1$).

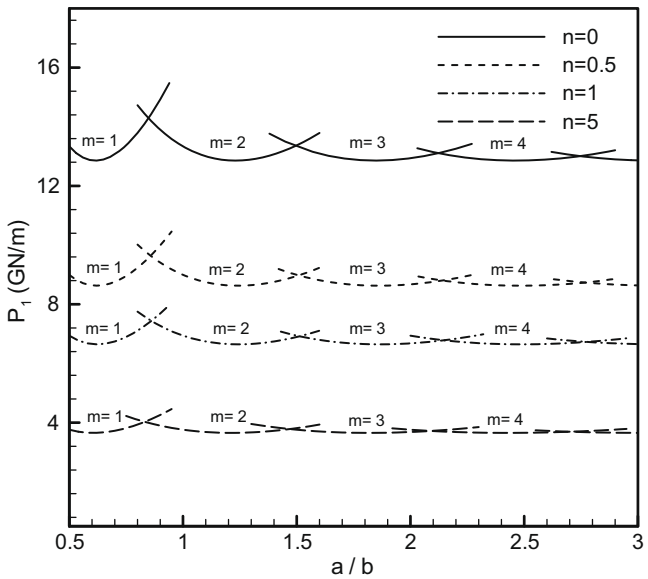

Fig. 3. The critical buckling load for a *SCSC* plate subjected to uniaxial compression along x direction versus the aspect ratio ($h/b = 0.2$).

and y directions. In Fig. 3, the critical buckling load versus the aspect ratio (a/b) is depicted for a *SCSC* plate subjected to uniaxial compression along x direction. As this figure shows, the number of half-waves in the x direction of critical buckling mode shape may change as the aspect ratio increases. All critical buckling modes have only one half-wave in the y direction. The effect of the aspect ratio for different kinds of loading conditions on the critical buckling load of a *SCSC* plate is presented in Fig. 4. It can be found that the buckling load generally decreases by increasing the aspect ratio. Also, the buckling load of the plate under uniaxial compression is greater than the one under biaxial compression and less than the one under biaxial compression and tension. The critical buckling mode shapes for three considered loading conditions have a single half-wave in the y direction. Moreover, it can be observed that the number of half-waves in the x direction of critical buckling mode shape of the FG pate under biaxial compression is varied slowly by increasing the aspect ratio.

The critical buckling load versus the thickness-side ratio (h/b) for a *SSSC* plate subjected to biaxial compression with different values of power of FGM is demonstrated in Fig. 5. It is observed that increasing the thickness of the FG plate severely

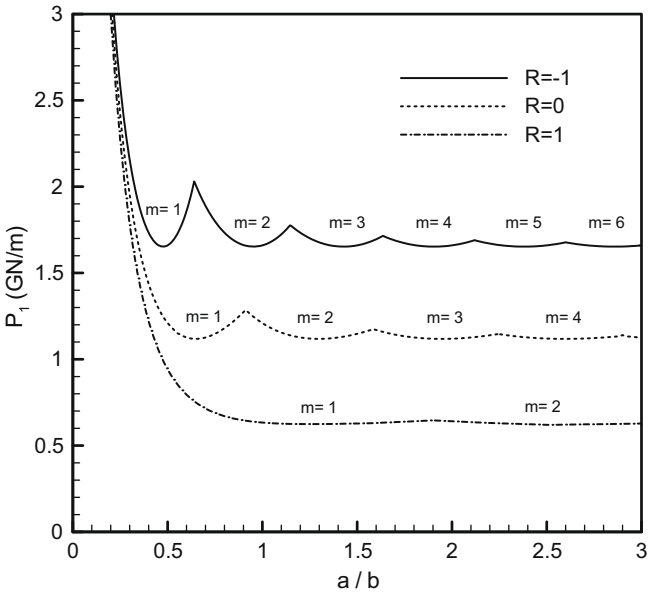

Fig. 4. Effect of the aspect ratio for different kinds of loading conditions on the critical buckling load of a *SCSC* plate $(h/b = 0.1,\ n = 1)$.

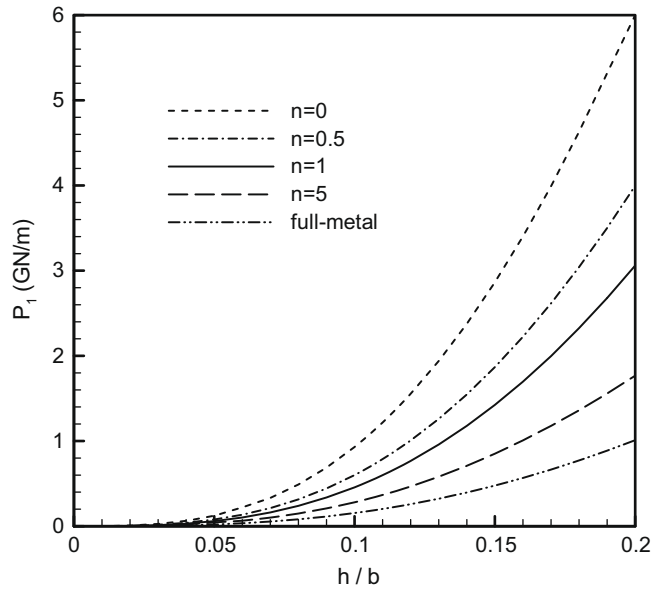

Fig. 5. The critical buckling load a *SSSC* plate under biaxial compression versus the thickness-side ratio $(a/b = 1)$.

increases the critical buckling load. Such behavior is due to the influence of the transverse shear deformation in the plate. Also, it can be concluded that in a specific thickness-side ratio, the critical buckling load of the FG plates is between those of full-ceramic and full-metal plates. It may be noted that the critical buckling mode shape of *SSSC* FG plate for all the thickness-side ratio and power of FGM considered in this figure have a single half-wave in the x and y direction.

The critical buckling loads have been tabulated in Tables 3–5 for the FG plates under uniaxial compression along the x axis, biaxial compression and biaxial compression and tension, respectively. These results are obtained for various boundary

Table 3
The critical buckling load $P_1(MN/m)$ for a functionally graded rectangular plate under uniaxial compression along the x axis with different boundary conditions in y direction.

n	$\frac{a}{b}$	$\frac{h}{b}$	Boundary condition					
			SCSC	*SSSC*	*SSSS*	*SCSF*	*SSSF*	*SFSF*
0	0.5	0.1	$2429.340^{(1)}$	$2232.1831^{(1)}$	$2079.721^{(1)}$	$1499.423^{(1)}$	$1470.693^{(1)}$	$1323.654^{(1)}$
		0.2	$13336.543^{(1)}$	$12702.371^{(1)}$	$12162.119^{(1)}$	$9113.010^{(1)}$	$8954.150^{(1)}$	$8150.561^{(1)}$
	1	0.1	$2429.340^{(2)}$	$1984.362^{(1)}$	$1437.361^{(1)}$	$594.405^{(1)}$	$509.626^{(1)}$	$350.863^{(1)}$
		0.2	$13336.543^{(2)}$	$12690.241^{(1)}$	$9915.620^{(1)}$	$4238.151^{(1)}$	$3693.266^{(1)}$	$2585.685^{(1)}$
	1.5	0.1	$2314.342^{(2)}$	$1851.590^{(2)}$	$1527.903^{(2)}$	$468.023^{(1)}$	$315.738^{(1)}$	$155.771^{(1)}$
		0.2	$13336.543^{(3)}$	$11508.194^{(2)}$	$10044.721^{(2)}$	$3304.235^{(1)}$	$2377.136^{(1)}$	$1199.691^{(1)}$
1	0.5	0.1	$1209.653^{(1)}$	$1107.261^{(1)}$	$1028.412^{(1)}$	$739.552^{(1)}$	$724.581^{(1)}$	$651.842^{(1)}$
		0.2	$6940.319^{(1)}$	$6576.342^{(1)}$	$6270.298^{(1)}$	$4598.421^{(1)}$	$4580.482^{(1)}$	$4161.171^{(1)}$
	1	0.1	$1209.653^{(2)}$	$975.175^{(1)}$	$702.304^{(1)}$	$289.923^{(1)}$	$248.830^{(1)}$	$170.563^{(1)}$
		0.2	$6940.319^{(2)}$	$6431.442^{(1)}$	$4955.431^{(1)}$	$2101.250^{(1)}$	$1826.052^{(1)}$	$1273.835^{(1)}$
	1.5	0.1	$1147.528^{(2)}$	$912.032^{(2)}$	$748.920^{(2)}$	$228.494^{(1)}$	$154.965^{(1)}$	$75.082^{(1)}$
		0.2	$6895.193^{(2)}$	$5863.120^{(2)}$	$5067.219^{(2)}$	$1697.295^{(1)}$	$1165.833^{(1)}$	$585.532^{(1)}$
2	0.5	0.1	$915.631^{(1)}$	$839.438^{(1)}$	$780.097^{(1)}$	$560.241^{(1)}$	$549.052^{(1)}$	$495.649^{(1)}$
		0.2	$5179.187^{(1)}$	$4915.543^{(1)}$	$4692.542^{(1)}$	$3482.043^{(1)}$	$3430.991^{(1)}$	$3124.761^{(1)}$
	1	0.1	$915.631^{(2)}$	$741.244^{(1)}$	$534.441^{(1)}$	$217.515^{(1)}$	$187.513^{(1)}$	$129.553^{(1)}$
		0.2	$5179.187^{(2)}$	$4841.131^{(1)}$	$3746.054^{(1)}$	$1551.974^{(1)}$	$1373.805^{(1)}$	$967.349^{(1)}$
	1.5	0.1	$869.563^{(2)}$	$692.329^{(2)}$	$569.751^{(2)}$	$171.345^{(1)}$	$116.267^{(1)}$	$57.647^{(1)}$
		0.2	$5161.429^{(2)}$	$4405.971^{(2)}$	$3819.109^{(2)}$	$1258.628^{(1)}$	$864.830^{(1)}$	$446.620^{(1)}$

The superscript numbers within the parenthesis indicate number of half-waves in the x direction.

Table 4
The critical buckling load $P_1(MN/m)$ for a functionally graded rectangular plate subjected to biaxial compression with different boundary conditions in y direction.

n	$\frac{a}{b}$	$\frac{h}{b}$	Boundary condition					
			SCSC	*SSSC*	*SSSS*	*SCSF*	*SSSF*	*SFSF*
0	0.5	0.1	$1893.975^{(1)}$	$1758.185^{(1)}$	$1663.777^{(1)}$	$1317.508^{(1)}$	$1311.309^{(1)}$	$1275.723^{(1)}$
		0.2	$10499.825^{(1)}$	$10061.967^{(1)}$	$9729.999^{(1)}$	$7890.382^{(1)}$	$7877.023^{(1)}$	$7769.795^{(1)}$
	1	0.1	$1282.278^{(1)}$	$930.725^{(1)}$	$718.692^{(1)}$	$404.082^{(1)}$	$377.944^{(1)}$	$340.818^{(1)}$
		0.2	$7679.962^{(1)}$	$6056.856^{(1)}$	$4957.888^{(1)}$	$2854.701^{(1)}$	$2711.786^{(1)}$	$2505.812^{(1)}$
	1.5	0.1	$1273.223^{(1)}$	$801.541^{(1)}$	$526.861^{(1)}$	$226.017^{(1)}$	$182.204^{(1)}$	$152.837^{(1)}$
		0.2	$7713.112^{(1)}$	$5337.452^{(1)}$	$3772.877^{(1)}$	$1653.361^{(1)}$	$1361.411^{(1)}$	$1175.134^{(1)}$
1	0.5	0.1	$941.649^{(1)}$	$871.255^{(1)}$	$822.738^{(1)}$	$651.075^{(1)}$	$647.747^{(1)}$	$629.283^{(1)}$
		0.2	$5456.902^{(1)}$	$5204.910^{(1)}$	$5016.384^{(1)}$	$4045.2008^{(1)}$	$4036.910^{(1)}$	$3973.591^{(1)}$
	1	0.1	$633.314^{(1)}$	$456.681^{(1)}$	$351.124^{(1)}$	$197.369^{(1)}$	$184.344^{(1)}$	$165.891^{(1)}$
		0.2	$3938.463^{(1)}$	$3060.183^{(1)}$	$2477.589^{(1)}$	$1417.198^{(1)}$	$1342.677^{(1)}$	$1235.1818^{(1)}$
	1.5	0.1	$628.045^{(1)}$	$392.608^{(1)}$	$256.776^{(1)}$	$110.151^{(1)}$	$88.648^{(1)}$	$74.179874^{(1)}$
		0.2	$3949.691^{(1)}$	$2685.255^{(1)}$	$1871.038^{(1)}$	$814.800^{(1)}$	$668.265^{(1)}$	$573.793460^{(1)}$
2	0.5	0.1	$713.124^{(1)}$	$660.516^{(1)}$	$624.158^{(1)}$	$494.038^{(1)}$	$491.578^{(1)}$	$477.782^{(1)}$
		0.2	$4073.489^{(1)}$	$3891.195^{(1)}$	$3754.274^{(1)}$	$3033.222^{(1)}$	$3027.360^{(1)}$	$2981.889^{(1)}$
	1	0.1	$480.647^{(1)}$	$347.326^{(1)}$	$267.416^{(1)}$	$150.327^{(1)}$	$140.470^{(1)}$	$126.494^{(1)}$
		0.2	$2952.8177^{(1)}$	$2305.460^{(1)}$	$1873.190^{(1)}$	$1073.771^{(1)}$	$1018.189^{(1)}$	$938.019^{(1)}$
	1.5	0.1	$476.842^{(1)}$	$298.763^{(1)}$	$195.714^{(1)}$	$83.9567^{(1)}$	$67.604^{(1)}$	$56.615^{(1)}$
		0.2	$2962.580^{(1)}$	$2025.799^{(1)}$	$1418.120^{(1)}$	$618.809^{(1)}$	$508.175^{(1)}$	$437.080^{(1)}$

The superscript numbers within the parenthesis indicate number of half-waves in the x direction.

Table 5
The critical buckling load $P_1(MN/m)$ for a functionally graded rectangular plate subjected to biaxial compression and tension along x and y direction with different boundary conditions in y direction.

n	$\frac{a}{b}$	$\frac{h}{b}$	Boundary condition					
			SCSC	*SSSC*	*SSSS*	*SCSF*	*SSSF*	*SFSF*
0	0.5	0.1	$3325.144^{(1)}$	$3023.619^{(1)}$	$2772.980^{(1)}$	$1637.782^{(1)}$	$1587.671^{(1)}$	$1334.640^{(1)}$
		0.2	$18026.631^{(1)}$	$17073.243^{(1)}$	$16216.712^{(1)}$	$9938.619^{(1)}$	$9650.849^{(1)}$	$8206.908^{(1)}$
	1	0.1	$3325.144^{(2)}$	$3023.619^{(2)}$	$2772.980^{(2)}$	$892.410^{(1)}$	$707.210^{(1)}$	$354.231^{(1)}$
		0.2	$18026.631^{(2)}$	$17073.243^{(2)}$	$16216.712^{(2)}$	$6230.543^{(1)}$	$5136.091^{(1)}$	$2616.870^{(1)}$
	1.5	0.1	$3325.144^{(3)}$	$3023.619^{(3)}$	$2772.980^{(3)}$	$1020.561^{(2)}$	$810.611^{(1)}$	$157.441^{(1)}$
		0.2	$17845.736^{(4)}$	$17073.243^{(3)}$	$16216.712^{(3)}$	$6831.130^{(2)}$	$6072.560^{(1)}$	$1213.210^{(1)}$
1	0.5	0.1	$1659.901^{(1)}$	$1501.320^{(1)}$	$1371.653^{(1)}$	$807.328^{(1)}$	$782.873^{(1)}$	$657.103^{(1)}$
		0.2	$9394.356^{(1)}$	$8846.942^{(1)}$	$8360.541^{(1)}$	$5086.517^{(1)}$	$4939.599^{(1)}$	$4192.873^{(1)}$
	1	0.1	$1659.901^{(2)}$	$1501.320^{(2)}$	$1371.653^{(2)}$	$435.541^{(1)}$	$344.564^{(1)}$	$172.301^{(1)}$
		0.2	$9394.356^{(2)}$	$8846.942^{(2)}$	$8360.541^{(2)}$	$3100.640^{(1)}$	$2540.051^{(1)}$	$1288.684^{(1)}$
	1.5	0.1	$1659.901^{(3)}$	$1501.320^{(3)}$	$1371.653^{(3)}$	$498.871^{(2)}$	$394.710^{(1)}$	$76.421^{(1)}$
		0.2	$9394.356^{(3)}$	$8846.942^{(3)}$	$8360.541^{(3)}$	$3468.901^{(2)}$	$2994.712^{(1)}$	$592.205^{(1)}$
2	0.5	0.1	$1255.638^{(1)}$	$1137.591^{(1)}$	$1040.519^{(1)}$	$609.112^{(1)}$	$593.715^{(1)}$	$499.429^{(1)}$
		0.2	$7009.320^{(1)}$	$6611.825^{(1)}$	$6257.811^{(1)}$	$3781.657^{(1)}$	$3680.982^{(1)}$	$3146.816^{(1)}$
	1	0.1	$1255.638^{(2)}$	$1137.591^{(2)}$	$1040.519^{(2)}$	$327.028^{(1)}$	$260.284^{(1)}$	$131.400^{(1)}$
		0.2	$7009.320^{(2)}$	$6611.825^{(2)}$	$6257.811^{(2)}$	$2294.502^{(1)}$	$1885.763^{(1)}$	$978.487^{(1)}$
	1.5	0.1	$1255.638^{(3)}$	$1137.591^{(3)}$	$1040.519^{(3)}$	$375.182^{(2)}$	$300.611^{(1)}$	$58.323^{(1)}$
		0.2	$7006.439^{(4)}$	$6611.825^{(3)}$	$6257.811^{(3)}$	$2572.761^{(2)}$	$2232.432^{(1)}$	$451.201^{(1)}$

The superscript numbers within the parenthesis indicate number of half-waves in the x direction.

conditions and loading conditions, some power of FGM and different thickness-side and aspect ratios. The critical buckling mode shapes for all six considered boundary conditions subjected to three loading conditions within the range of a/b and h/b given in Tables 3–5 have a single half-wave in the y direction.

From the results presented in these tables, it can be easily observed that, as the thickness-side ratio increases from 0.1 to 0.2, the critical buckling load increases. Moreover, it can be seen that increasing the thickness-side ratio not only increases the values of the critical buckling load, but also causes changes in the numbers of half-waves in the x direction of critical buckling mode shape. As an example, for a *SCSC* plate subjected to biaxial compression and tension with aspect ratio $(a/b = 1.5)$ and power of FGM equal to 0 or 2, the number of half-waves in the x direction of critical buckling mode shape varies from 3 to 4 as the values of thickness-side ratio increases from 0.1 to 0.2. Inspecting data given in Table 4 observes that in the case of biaxial compression the plate the critical buckling mode have a single half-wave in x and y directions for the presented aspect and thickness-side ratios. Also, according to Tables 3 and 5, it is observed that for some boundary conditions by increasing the aspect ratio, the critical buckling load remains in the constant value, whereas the numbers of half-waves in the x direction of critical buckling mode shape increases. For example, in the Table 5, $P_1 = 1371.653$ is the critical buckling load of a *SSSS* plate with $(n = 1,\ h/b = 0.1)$ and $(a/b = 0.5, 1, 1.5)$. This is because the parameter λ_m is appear in determinate of coefficient matrix, and while the parameters m and a selected in which their ratio be a constant value, the buckling load dose not change. Thus in the above case the parameter λ_m may be given as

$$\lambda_m = \frac{m\pi}{a} = \frac{1\pi}{0.5} = \frac{2\pi}{1} = \frac{3\pi}{1.5} = \cdots \tag{49}$$

It should be noted that among the identical buckling loads, some of them may be the critical buckling load. Inspection of Tables 3–5 also indicates that, the lowest and highest values for critical buckling loads are corresponding to *SFSF* and *SCSC* cases, respectively. Thus, the constraints at the edges increase the stiffness of the FG plate, which results in a higher critical buckling load.

8. Conclusion

In the present article, an analytical method has been developed for buckling analysis of thick functionally graded rectangular plates. Based on the higher-order shear deformation plate theory, the equilibrium and stability equations have been obtained. Using an analytical approach, the governing stability equations of functionally graded rectangular plates have been decoupled and converted into two independent equations in terms of transverse displacement and boundary layer function. Solving the decoupled equations, the Levy-type solution has been presented for functionally graded rectangular plates with two opposite edges simply supported. The influences of power of functionally graded material, aspect ratio, thickness-side ratio, loading conditions and different combinations of boundary conditions on the critical buckling load of the functionally

graded rectangular plates have been studied. The success of the present analysis has been also verified through comparisons with available results for thin and simply supported thick functionally graded rectangular plates.

Appendix A

In order to derive Eqs. (25a), (23a) and (23b) are differentiated with respect to y and x, respectively, and finally the two results are subtracted. Also, for deriving Eqs. (25b), (23a) and (23b) are differentiated with respect to x and y, respectively, and then adding the result, the following relation is obtained:

$$\widehat{C}\Delta^2\varphi_3 - \widehat{A}(\varphi_3 + \Delta^2 w^1) - \widehat{H}\Delta^4 w^1 = 0. \tag{A-1}$$

Eliminating the term $\nabla^2\varphi_3$ from Eqs. (23c) and (A-1) yields

$$\varphi_3 = \frac{\widehat{F}\widehat{C} - \widehat{H}^2}{\widehat{A}(\widehat{C} + \widehat{H})}\nabla^4 w^1 - \nabla^2 w^1 - \frac{\widehat{C}}{\widehat{A}(\widehat{C} + \widehat{H})}\left(N^0_{xx}w^1_{,xx} + 2N^0_{xy}w^1_{,xy} + N^0_{yy}w^1_{,yy}\right). \tag{A-2}$$

By substituting Eq. (A-2) into Eq. (23c), the interior Eq. (25b) is obtained.
Also, the Eqs. (23a) and (23b) can be rewritten as

$$\psi_x = \frac{\widehat{C}}{\widehat{\widehat{A}}}\varphi_{3,x} + \frac{\widehat{B}}{\widehat{\widehat{A}}}\varphi_{4,y} - \frac{\widehat{H}}{\widehat{\widehat{A}}}\nabla w^1_{,x} - w^1_{,x}, \tag{A-3}$$

$$\psi_y = \frac{\widehat{C}}{\widehat{\widehat{A}}}\varphi_{3,y} - \frac{\widehat{B}}{\widehat{\widehat{A}}}\varphi_{4,x} - \frac{\widehat{H}}{\widehat{\widehat{A}}}\nabla w^1_{,y} - w^1_{,y}. \tag{A-4}$$

By substituting Eq. (A-2) into the above equations, Eq. (27) can be obtained.

References

[1] J.N. Reddy, A simple higher-order theory for laminated composite plates, J. Appl. Mech. 51 (1984) 745–752.
[2] J.N. Reddy, Analysis of functionally graded materials, Int. J. Numer. Meth. Eng. 47 (2000) 663–684.
[3] L.S. Ma, T.J. Wang, Relationships between axisymmetric bending and buckling solutions of FGM circular plates based on third-order plate theory and classical plate theory, Int. J. Solids Struct. 41 (2004) 85–101.
[4] R. Javaheri, M.R. Eslami, Buckling of functionally graded plates under in-plane compressive loading, ZAMM 82 (4) (2002) 277–283.
[5] M.M. Najafizadeh, H.R. Heydari, Thermal buckling of functionally graded circular plates based on higher order shear deformation plate theory, Eur. J. Mech. A/Solid. 23 (2004) 1085–1100.
[6] M.M. Najafizadeh, H.R. Heydari, An exact solution for buckling of functionally graded circular plates based on higher order shear deformation plate theory under uniform radial compression, Int. J. Mech. Sci. 50 (2008) 603–612.
[7] A.J.M. Ferreira, R.C. Batra, C.M.C. Roque, L.F. Qian, P.A.L.S. Martins, Static analysis of functionally graded plates using third-order shear deformation theory and a meshless method, Compos. Struct. 69 (2005) 449–457.
[8] B.A. Samsam Shariat, M.R. Eslami, Buckling of thick functionally graded plates under mechanical and thermal loads, Compos. Struct. 78 (2007) 433–439.
[9] A.M. Zenkour, Generalized shear deformation theory for bending analysis of functionally graded plates, Appl. Math. Modell. 30 (2006) 67–84.
[10] A.R. Saidi, A. Rasouli, S. Sahraee, Axisymmetric bending and buckling analysis of thick functionally graded circular plates using unconstrained third-order shear deformation plate theory, Compos. Struct. 89 (2009) 110–119.
[11] M. Levy, Memoire sur la theorie des plaques elastiques planes, J. Math. Pure. Appl. 3 (1899) 219–306.
[12] R. Szilard, Theory and Analysis of Plates, Prentice-Hall, Englewood Cliffs, NJ, 1974.
[13] A.C. Ugural, Stresses in Plates and Shells, McGraw-Hill, New York, 1981.
[14] D.W. Cooke, M. Levinson, Thick rectangular plates – II. The generalized levy solution, Int. J. Mech. Sci. 25 (3) (1983) 207–215.
[15] J.N. Reddy, Energy Principles and Variational Methods in Applied Mechanics, John Wiley, New York, 1984.
[16] J.N. Reddy, A.A. Khdeir, L. Librescu, Levy type solutions for symmetrically laminated rectangular plates using first-order shear deformation theory, J. Appl. Mech. 54 (1987) 740.
[17] R.F. Palardy, A.N. Palazotto, Buckling and vibration of composite plates using the levy method, Compos. Struct. 14 (1990) 61–86.
[18] W.C. Chen, W.H. Liu, Thermal buckling of antisymmetric angle-ply laminated plates – an analytical Levy-type solution, Therm. Stress. 16 (4) (1993) 401–419.
[19] A.S. Oktem, R.A. Chaudhuri, Levy type analysis of cross-ply plates based on higher-order theory, Compos. Struct. 78 (2007) 243–253.
[20] A. Nosier, J.N. Reddy, On vibration and buckling of symmetric laminated plates according to shear deformation theories: part I, Acta Mech. 94 (1992) 123–144.
[21] A. Nosier, J.N. Reddy, On vibration and buckling of symmetric laminated plates according to shear deformation theories: part II, Acta Mech. 94 (1992) 145–169.
[22] E. Jomehzadeh, A.R. Saidi, S.R. Atashipour, An analytical approach for stress analysis of functionally graded annular sector plates, J. Mater. Des. 30 (2009) 3679–3685.
[23] A.R. Saidi, E. Jomehzadeh, On analytical approach for the bending/stretching of linearly elastic functionally graded rectangular plates with two opposite edges simply supported, J. Mech. Eng. Sci. 223 (2009) 2009–2016.
[24] S.R. Atashipour, A.R. Saidi, E. Jomehzadeh, On the boundary layer phenomenon in bending of thick annular sector plates using third-order shear deformation theory, Acta Mech. 211 (2009) 89–99.
[25] M. Mohammadi, A.R. Saidi, E. Jomehzadeh, Levy solution for buckling analysis of functionally graded rectangular plates, Appl. Compos. Mater. 17 (2010) 81–93.
[26] G.N. Praveen, J.N. Reddy, Nonlinear transient thermoelastic analysis of functionally graded ceramic–metal plates, Int. J. Solids Struct. 35 (1998) 4457–4476.
[27] S. Chi, Y. Chung, Mechanical behavior of functionally graded material plates under transverse load – part I: analysis, Int. J. Solids Struct. 43 (2006) 3657–3674.
[28] D.O. Brush, B.O. Almroth, Buckling of Bars, Plates, and Shells, McGraw-Hill, New York, 1975.